Journal of Optoelectronics and Advanced Materials Vol. 7, No. 2, April 2005, p. 589 - 598

Invited Paper

GIANT MAGNETORESISTANCE IN ELECTRODEPOSITED MULTILAYER FILMS. THE INFLUENCE OF SUPERPARAMAGNETIC REGIONS

I. Bakonyi[a]*, L. Péter[a], V. Weihnacht[a#], J. Tóth[a], L. F. Kiss[a], C. M. Schneider[b§]

[a]Research Institute for Solid State Physics and Optics, Hungarian Academy of Sciences H-1525 Budapest, P.O.B. 49, Hungary
[b]Leibniz Institute for Solid State Physics and Materials Research (IFW), Dresden, Germany

When preparing an alternating sequence of magnetic (Co or Ni) and non-magnetic (Cu) layers by electrodeposition using the two-pulse plating technique, a dissolution of the less-noble magnetic Co and Ni atoms can take place during the deposition of the more noble and non-magnetic Cu atoms. This process results in changes of the actual sublayer thicknesses with respect to the nominal values and can also cause some chemical intermixing at the magnetic/non-magnetic interfaces. As a consequence, superparamagnetic (SPM) regions with "loose magnetic moments" can form as has been demonstrated for electrodeposited Ni-Cu/Cu multilayers. We have also shown recently for electrodeposited Co-Cu/Cu multilayers that if some fraction of the magnetic layers exhibits SPM behaviour then the observed giant magnetoresistance (GMR) can be quantitatively decomposed into a ferromagnetic (FM) and a SPM contribution. In this paper, the results of a similar GMR decomposition study are presented for two electrodeposited Co-Cu/Cu multilayers. In the multilayer with strongly non-saturated magnetoresistance curves, the dominant GMR term was due to SPM regions, whereas in the other multilayer for which the magnetoresistance is mostly saturated in magnetic fields around 1 to 2 kOe, the FM contribution to the GMR is much larger. At the same time, magnetic measurements on the first multilayer sample have also revealed the presence of a large SPM contribution to the magnetization.

(Received August 18, 2004; accepted March 23, 2005)

Keywords: Giant magnetoresistance (GMR), Superparamagnetism (SPM), Electrodeposited multilayers

1. Introduction

In metallic magnetic nanostructures, spin-dependent scattering phenomena occur when conduction electrons travel between two magnetic regions through a non-magnetic spacer material [1]. These phenomena can be interpreted in the framework of the established two-band model of metallic ferromagnets [2]. On the basis of this model, the resistivity contribution due to spin-dependent scattering along an electron path "magnetic region 1 → non-magnetic region → magnetic region 2" depends on the mutual orientation of the magnetizations in the two magnetic regions [3]. Typically, this resisitivity contribution is maximum when the two magnetizations are antiparallel to each other and minimum when they are parallel. The spin-dependent scattering events result in the so-called giant magnetoresistance (GMR) effect [1,3-5].

Magnetic nanostructures exhibiting such spin-dependent phenomena can be grouped into multilayers and granular materials. A typical multilayer consists of a stack of layers of a magnetic

* Corresponding author: bakonyi@szfki.hu
# On leave from the Leibniz Institute for Solid State Physics and Materials Research (IFW), Dresden, Germany. Present address: Fraunhofer Institute for Material and Beam Technology, Dresden, Germany.
§ Present address: Institute of Solid State Research IFF-6, Research Center Jülich, Germany

metal or alloy separated by a non-magnetic (Pauli paramagnetic) metal. At appropriate spacer thicknesses it exhibits GMR [4,6-8]. In granular magnetic nanostructures where nanosized magnetic particles are embedded in a non-magnetic metallic matrix, similarly to multilayers GMR can occur at appropriate average distances between the nanoparticles [9-11].

In magnetic/non-magnetic multilayers, the magnetic layers usually exhibit ferromagnetic (FM) behaviour, whereas for the granular nanostructures the magnetic entities are typically so small that they exhibit superparamagnetic (SPM) characteristics. The latter behaviour occurs, if the size of a FM object assumed to be in a single-domain state is reduced to the extent that the total magnetic anisotropy energy KV (where K is the anisotropy constant and V is the object's volume) falls below the thermal energy k_BT [12]. It is customary to define a blocking temperature T_B by the relation $KV = 25\ k_BT_B$ [12]. For a given volume of the magnetic object, below the blocking temperature ($T < T_B$), i.e. without sufficient thermal excitations, the magnetization orientation is fixed along one of the easy axes in zero external magnetic field and FM characteristics can be observed upon the application of a magnetic field. Above the blocking temperature ($T > T_B$), the magnetization orientation rapidly fluctuates due to thermal excitations. An assembly of non-interacting SPM objects is characterised by zero remanence and vanishing hysteresis (zero coercive field, H_C).

As a consequence of the difference in the characteristics of the magnetic components in the layered and the granular magnetic/non-magnetic metallic nanostructures, their magnetic and magnetoresistance (MR) behaviour also differs. For layered structures prepared by physical deposition methods, usually a clear antiferromagnetic (AF) coupling between the neighbouring FM layers through the spacer can be observed [5], and both the coupling strength and the GMR magnitude oscillate with spacer layer thickness [1,6-8]. The AF coupling strength is determined at the MR saturation, which typically occurs in magnetic fields of a few kOe [6-8]. At low spacer layer thicknesses, the MR curves in general exhibit no hysteresis, whereas at thick spacers their typical characteristics is a splitting of the MR curves with sharp peaks, the latter feature being indicative of weak or vanishing interlayer coupling [13]. In granular systems, the SPM particles are randomly distributed in space and there is usually negligible coupling between their magnetic moments. The field dependence of the magnetization of such a system is described by the Langevin function L(x) [12], where $x = \mu H/k_BT$ with μ as the average magnetic moment of the SPM particles (it is customary to write $\mu = N\mu_B$, where μ_B is the Bohr magneton and then N can be used as a parameter characterizing the average macrospin of the particle). Since the probability of spin-dependent scattering depends on the relative orientation of the magnetic moments of the two magnetic particles involved in the scattering process (magnetic regions 1 and 2 as discussed above), an appropriate thermal average of the magnetic moment orientations should be considered. It has been shown [14,15,16] that for uncorrelated SPM magnetic moments, this leads to a field dependence of the magnetoresistance, MR(H), which is proportional to the square of the magnetization, i.e., $MR(H) \propto [L(x)]^2$. This relation has indeed been observed in many granular alloys [10,11]. The magnetization saturation of SPM particles usually occurs in magnetic fields of several tens of kOe and, consequently, the MR curves were also found to approach saturation in very high magnetic fields only.

However, it has also been observed for some granular alloys [17-19], that the $MR(H) \propto [L(x)]^2$ relation does not always properly describe the experimental MR data. This was explained on the basis of a model elaborated by Wiser [16] and Hickey et al. [17], assuming that a wide range of particle sizes is present so that a significant fraction of the larger particles already exhibits FM behaviour at a given temperature. In the presence of both SPM and FM particles this model requires to distinguish between three cases for the spin-dependent scattering events along an electron path of the type "magnetic region 1 → non-magnetic region → magnetic region 2". The three cases are as follows: (i) both magnetic particles are SPM; (ii) both magnetic particles are FM, and (iii) one of the magnetic particles is SPM, while the other is FM. Each of these three cases contributes in a unique manner to the field dependence of the magnetoresistance, MR(H), for the following reason. For a SPM particle, a large magnetic field is needed to align its magnetic moment. By contrast, the moment of a FM particle is aligned in a much smaller magnetic field, typically a few kOe. Case (i) corresponds to a conventional granular metal with SPM particles only, for which

$MR(H) \propto [L(x)]^2$ [14,15,16]. For case (ii), the moments of both FM particles are aligned at relatively small fields ($H_S \approx 2$ kOe) and the magnetic field has then no further effect on the resistivity. Therefore, above the relatively small saturation field of the FM particles scattering along an electron path "FM particle 1 → non-magnetic region → FM particle 2" does not contribute to the MR. For case (iii), i.e., for an electron path "SPM particle → non-magnetic region → FM particle" or "FM particle → non-magnetic region → SPM particle", the situation is different. The moment of the FM particle is already aligned at higher magnetic fields, and the correlation of the two magnetic moments involved in the scattering process depends on the time average of the spatial orientation of the SPM particle moment only. This was shown [16,17] to lead to a linear dependence of the magnetoresistance on the SPM magnetization for high fields, i.e., $MR(H) \propto L(x)$. Appropriate expressions were derived in Ref. [16] in the presence of all three types of scattering scenarios, also for a distribution of magnetic particle sizes.

The results discussed above refer to an extension of the conventional granular alloy situation containing SPM particles to the case when also FM particles must be considered. It has been shown recently [20-22], however, that in some cases the conventional picture of magnetic/non-magnetic multilayers with purely FM layers must also be extended in an appropriate manner, i.e., by taking into account the presence of SPM regions in the layer stacking.

It turned out from a quantitative analysis of GMR data obtained from electrodeposited Co-Cu/Cu multilayers [22], that beyond the technical saturation of the FM component at about $H_S = 1.7$ kOe, the field dependence of both the magnetization M(H) and the MR(H) can be described by the Langevin function L(x). In terms of the Wiser-Hickey model [16,17], this means that in these Co-Cu/Cu multilayers the GMR arises from spin-dependent scattering of electrons which travel through the non-magnetic spacer between two FM regions (GMR_{FM}) or between a FM region and a SPM region (GMR_{SPM}), whichever is the first or second. We can visualize the magnetic layers in such multilayers as being broken up into FM and SPM regions due to the specific growth conditions, whereby the SPM regions are decoupled from the FM regions of the magnetic layers. From subsequent scattering events within a FM region, also an anisotropic magnetoresistance (AMR) contribution [23] can arise, that indistinguishably adds to the GMR_{FM} term for $H > H_S$. In this manner, for magnetic fields $H > H_S = 1.7$ kOe we can describe the MR(H) data in the form

$$MR(H) = MR_{FM} + GMR_{SPM}\, L(x), \tag{1}$$

whereby $MR_{FM} = AMR + GMR_{FM}$ is a constant term. The relative weight of the MR_{FM} and the GMR_{SPM} terms as well as that of the two contributions in MR_{FM} (AMR and GMR_{FM}) do not simply depend on the volume fractions of the two kinds of magnetic regions, since these weights are also determined by the scattering probability in the different regions as well as other factors related to the mutual spatial distribution and also the morphology of the FM, SPM and non-magnetic regions.

Recently, we have reported [24] on a room-temperature MR study of electrodeposited Co-Cu/Cu multilayers prepared under much more controlled conditions than in Ref. 22 in order to reveal the influence of deposition conditions on the MR characteristics in more detail. The present paper aims at an analysis of the results from two selected samples reported in Ref. 24 by decomposing the FM and SPM magnetoresistance contributions according to the method described in Ref. 22. In addition, for one of these samples, magnetization measurements were also performed in order to separate the individual FM and SPM magnetic contributions and to compare them to the corresponding GMR terms. In particular, the role of the Co dissolution process taking place during the mass-transport limited Cu deposition in the multilayer growth and the SPM region formation, as well as the consequences of these features on the MR characteristics will be discussed.

2. Experimental

2.1 Sample preparation and chemical analysis

The sample preparation has been described previously [24]. An aqueous electrolyte with two solutes ($CoSO_4$ and $CuSO_4$) was used to prepare magnetic/non-magnetic Co-Cu/Cu multilayers by the two-pulse plating technique. Electrodeposition was performed in a tubular cell ensuring a lateral homogeneity of the deposition current density over the cathode area. A polished Ti foil placed at the bottom of the cell served as cathode. After deposition, the multilayers with a bilayer number of 300 were peeled off mechanically from the Ti sheet. A galvanostatic/potentiostatic (G/P) pulse sequence was employed, by means of which the Co-rich magnetic Co-Cu layers (often referred to as Co layers) were deposited by current control and the non-magnetic Cu layers by potential control.

The magnetic layer consisting of a $Co_{95}Cu_5$ alloy [25] was deposited at 35 mA/cm^2 cathodic current density. The non-magnetic layer (Cu) was deposited at –0.25 V potential with respect to a saturated calomel electrode (SCE). During both pulses, the total charge deposited was monitored by a computer-controlled data acquisition system. The layer thickness was controlled with the pulse lengths and from the charge deposited during the pulse, the nominal layer thickness was determined. For the present study, two samples with the same nominal magnetic layer thickness, but with very different nominal non-magnetic layer thickness were selected. The nominal thickness of the two samples (codes V4 and V6) are given in the second column of Table 1.

In Ref. 24, the overall chemical composition of several Co-Cu/Cu multilayers was measured with electron probe microanalysis (EPMA). From the analysis results, we deduced the actual effective layer thicknesses by taking into account that the magnetic layer composition is $Co_{95}Cu_5$ and the non-magnetic layer is pure Cu. For sample V4, the actual layer thicknesses as given in the last column of Table 1 were obtained. These data indicate a decrease of the magnetic layer thickness by 1.4 nm with respect to the nominal value and an increase by the same amount for the non-magnetic layer thickness. Since the layer thickness change was similarly (1.4 nm for two other samples prepared at the same Cu deposition potential), we may take the same change for sample V6 as well and the actual layer thicknesses estimated in this manner are also specified in Table 1.

Table 1. Nominal layer thicknesses as determined from the deposition parameters and actual layer thicknesses as derived from the EPMA analysis results [24] for the two Co-Cu/Cu multikayer samples selected for the present study.

multilayer sample code	nominal layer thicknesses (magnetic/non-magnetic)	layer thicknesses determined from EPMA (magnetic/non-magnetic)
V4	3.4 nm/0.2 nm	2.0 nm/1.6 nm
V6	3.4 nm/2.5 nm	≈2.0 nm/≈3.9 nm

The 1.4 nm difference between the nominal and actual layer thicknesses is substantial and the explanation for this phenomenon is the dissolution of the previously deposited less noble Co atoms [26], which accompanies the deposition of the more noble Cu atoms both processes taking place randomly over the cathode area. Similar thickness changes by the same mechanism have been reported for electrodeposited Ni-Cu/Cu multilayers as well [27].

2.2 Measurement of magnetoresistance and magnetic properties

The MR was measured on 1 to 2 mm wide strips at room temperature with the four-point-in-line method in magnetic fields between –8 kOe and +8 kOe in the field-in-plane/current-in-plane geometry. Both the longitudinal (LMR) and the transverse (TMR) magnetoresistance (field parallel to current and field perpendicular to current, respectively) components were recorded for each sample. The following formula was used for calculating the magnetoresistance ratio: $\Delta R/R_0 = [R(H) - R(0)]/R(0)$ where R(H) is the resistance in the magnetic field H and R(0) is the resistance when H = 0.

A SQUID magnetometer was used to measure the in-plane magnetization curves at 300 K up to H = 50 kOe on the same strip of sample V4, which was used for the MR measurements.

3. Results

3.1 Magnetoresistance

The longitudinal magnetoresistance (LMR) data for the Co-Cu/Cu multilayer sample V4 is shown in Fig. 1a by the symbols ■. Fig. 1a indicates the decomposition method for fitting the MR(H) data as described in Ref. 22. For magnetic fields above about H_S = 1.7 kOe, the MR data could be well fitted by a Langevin function L(x) (dashed line in Fig. 1a), representing the SPM contribution GMR_{SPM} to the magnetoresistance. By subtracting the fitted Langevin function from the experimental data, the FM component, MR_{FM}, to the magnetoresistance was obtained (solid line).

Fig. 1b shows the decomposed MR_{FM} and GMR_{SPM} terms for both the longituidnal and transverse components of sample V4. It can be clearly seen, that the total MR is dominated by the non-saturating SPM contribution. The negative values of the LMR and TMR components for both the MR_{FM} and GMR_{SPM} terms indicate a clear GMR effect. The average magnetic moment of a SPM regions as deduced from the Langevin fit is about 4000 μ_B.

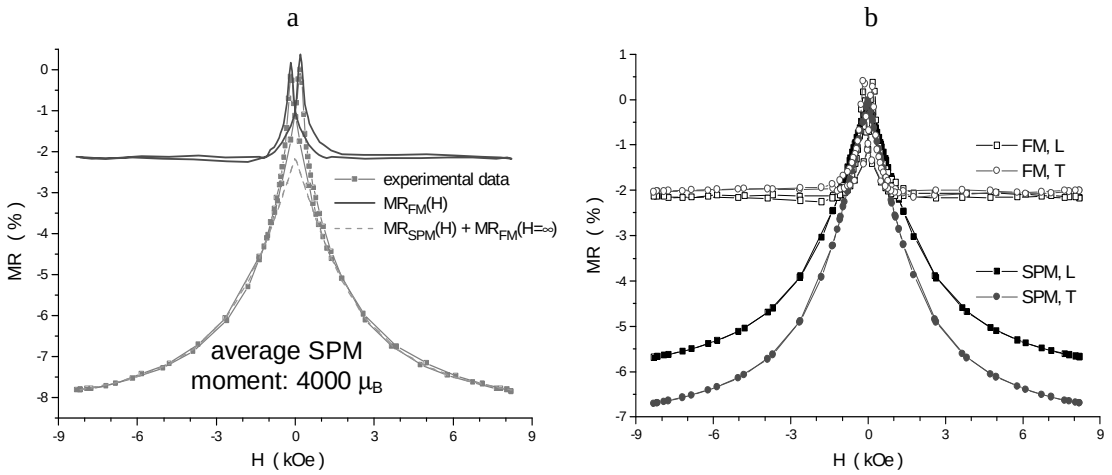

Fig. 1. Decomposition of the room-temperature MR curves for multilayer sample V4: (a) measured LMR data (symbols ■) and decomposed FM (solid line) and SPM (dashed line) contributions to the observed magnetoresistance; (b) decomposed FM (open symbols) and SPM (solid symbols) contributions to the observed magnetoresistance for both the longitudinal (L) and transverse (T) components. The SPM term dominates over the FM term. The size of the average SPM magnetic moment as deduced from the Langevin fit according to eq. (1) is also indicated.

For the multilayer sample V6, the same data and analysis results are displayed in Fig. 2. In contrast to sample V4 (see Fig. 1), we now find a dominance of the GMR_{FM} term in the total measured magnetoresistance. For this sample, the average magnetic moment of a SPM region as deduced from the Langevin fit is about 7000 μ_B. This value is nearly twice that obtained for sample V4.

In terms of the Wiser-Hickey model [16,17] as described in the Introduction, we can now deduce that in multilayer sample V6 the magnetic layers consist of mainly FM regions with a small SPM fraction being magnetically decoupled from the FM regions, whereas the situation is reversed for sample V4. There was no need to include a $[L(x)]^2$ term in fitting the experimental data, which would account for spin-dependent scattering along electron paths "SPM region 1 → non-magnetic region → SPM region 2".

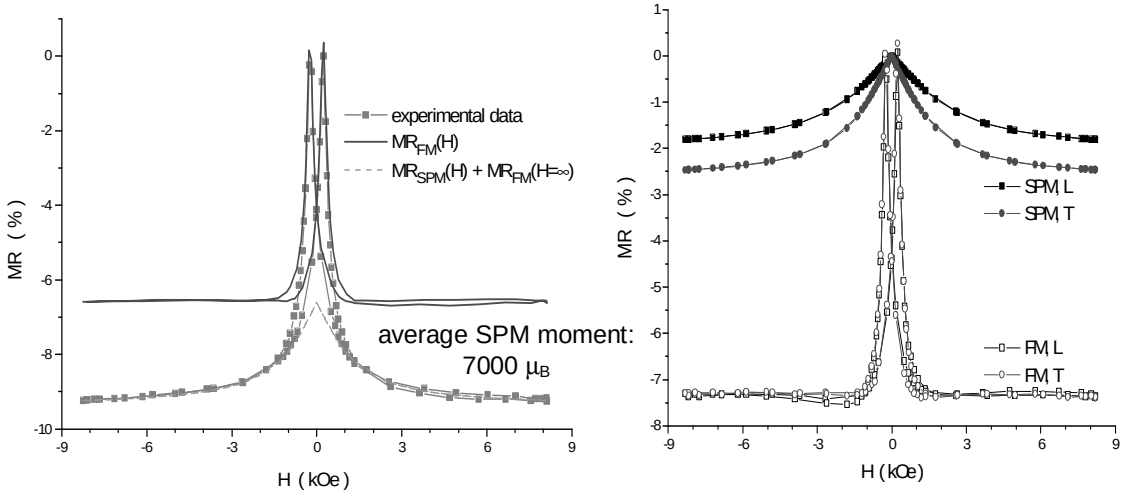

a b

Fig. 2. The same analysis of the room-temperture MR data for multilayer sample V6 as shown for sample V4 in Fig. 1. For sample V6, the FM term dominates over the SPM term. The size of the average SPM magnetic moment as deduced from the Langevin fit according to eq. (1) is also indicated and it is nearly twice as large as for sample V4 (see Fig. 1).

3.2 Magnetic properties

The magnetic hysteresis loop of sample V4 is shown in Fig. 3. Since the saturation value of the magnetization is about 160 emu/g, we can see that about 80 % of the magnetization (i.e., the value at that magnetic field where the hysteresis loop closes) originates from the FM parts of the magnetic layer. The rest of the saturation magnetization is due to the alignment of the SPM regions. With reference to Fig. 1, we conclude that the ratio of the SPM and FM contributions is about 3:1 for the GMR and about 1:4 for the magnetization. This very large difference is due to the fact that the magnetization ratio is determined by the volume fractions of the two components only, whereas for the GMR the magnitudes of the FM and SPM contributions also depend strongly on the mutual spatial arrangement of the two kinds of regions. Moreover, GMR is mainly governed by electron transitions across magnetic/non-magnetic interfaces.

The high-field saturation magnetization of sample V4, as determined for the unit mass of the magnetic layer by using the magnetic layer thickness derived from the chemical analysis (see Section 2.1), is fairly close to the saturation magnetization of pure Co metal. By even taking into account the slight Cu-content in the magnetic layer (composition: $Co_{95}Cu_5$), this means that the sublayer thicknesses (Table 1) calculated from the chemical analysis results should be fairly close (within about 10 %) to the actual layer thicknesses.

As in our other recent study of electrodeposited Co-Cu/Cu multilayers [28], the coercive field of multilayer V4 was found to be much higher than the value for bulk electrodeposited $Co_{95}Cu_5$ alloys. This can be attributed to thin film effects [28], indicating that the magnetic layers in multilayer V4 are indeed in the nanometer thickness range.

The high-field magnetization measurements of sample V4 provided data for a sufficient range of magnetic fields and made it possible to perform a Langevin fit also for the magnetization, similarly as in eq. (1) for the magnetoresistance. This fit yielded an average magnetic moment value for the SPM regions, which was is in excellent agreement with the SPM moment size derived from the MR data for sample V4.

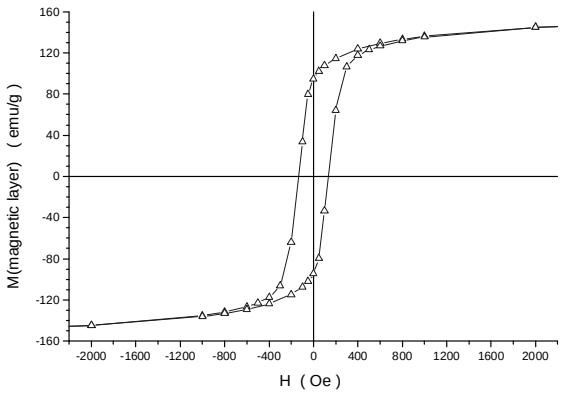

Fig. 3. Room-temperature magnetic hysteresis loop for multilayer sample V4 with the magnetization referred to the unit mass of the magnetic layer only. The coercive field is approximately the same as the magnetic field at which the MR peak occurs. It can be observed that the FM component of the magnetization saturates above about 1 kOe (closing of the hystersis loop). The saturation magnetization in high magnetic fields (50 kOe) is about 160 emu/g, the increase of M to this value from the data shown in the figure up to 2 kOe results from the contribution of SPM regions.

4. Discussion

According to the results described in Section 3, multilayers V4 and V6 exhibit very different GMR field dependences in spite of the fact that their GMR values as measured in a magnetic field of 8 kOe are very similar. The explanation of the observed differences should be sought in the details of the underlying electrochemical processes governing the multilayer growth.

For multilayer V4 (nominal magnetic/non-magnetic layer thickness: 3.4 nm/0.2 nm), the Cu layer with a final thickness of 1.6 nm (Table 1) is built up almost exclusively during the dissolution period of the previously deposited magnetic Co-Cu layer (the latter being reduced, on the average, down to a thickness of about 2 nm). Such a consumption of the magnetic layer occurs randomly over the cathode area and this leads to a strong local fluctuation of the magnetic layer thickness. Although the large observed GMR indicates that the non-magnetic spacer layer (Cu) is probably continuous (absence of FM coupling via pin-holes), the relatively small total Cu thickness certainly means that the Cu layer covers the magnetic layer more or less homogeneously, i.e., the Cu layer surface conformally maps the large surface roughness of the magnetic layer.

On the other hand, for multilayer V6 (nominal magnetic/non-magnetic layer thickness: 3.4 nm/2.5 nm) it can be assumed that only less than half (1.4 nm) of the final Cu layer thickness (3.9 nm) is built up during the dissolution of the less-noble layer on top of which another thick Cu layer (2.5 nm) is deposited thereafter. This latter process may well lead to a “levelling” effect, i.e., the top surface of the thick Cu layer may be much smoother than in the case of the thinner Cu layer of sample V4. Therefore, the next magnetic layer may start to grow in the case of multilayer V6 on a smoother surface and may become more uniform. Although the Co dissolution consumes again nearly half of the next magnetic layer, this process may take place on the smoother surface of

multilayer V6 more uniformly and may result in much weaker layer thickness fluctuations. As a result, there is much lower probability for the formation of SPM regions. Indeed, we have obtained an average SPM moment about twice the size for sample V6 than for sample V4.

In this manner, we could give some reasonable arguments for explaining the difference in the observed GMR behaviour on the basis of the particular deposition parameters. The experimental data unambiguously reveal the presence of SPM regions in these multilayers, which are magnetically decoupled from the FM parts of the magnetic layers. However, it is not at all easy to determine the location of the magnetically separated SPM regions.

In a previous work [21], we have considered the SPM regions in electrodeposited $Ni_{81}Cu_{19}$ multilayers as small magnetic islands in the plane of the magnetic layers (see Fig. 7 of Ref. 21), whereby these islands are separated from the FM parts by a non-magnetic region. The Co dissolution process can lead to layer thickness fluctuations, which – at the extreme – can result in a complete dissolution of the magnetic layer at some places. Since solute Cu atoms strongly reduce the magnetization of Co metal, a strong Cu enrichment at some places of the magnetic layer can also result in the formation of non-magnetic regions. In this manner, we can imagine some processes leading to the formation of SPM islands.

Another possibility in accounting for an SPM contribution is to assume that such regions with "loose" magnetic moments leading to strongly non-saturated magnetoresistance curves are situated between the FM "core" of the magnetic layers and the non-magnetic layers. A sketch of such a situation is shown in Fig. 4, where the possible electron paths leading to spin-dependent scattering (a GMR effect) are also specified. At low magnetic fields, both FM → SPM (or SPM → FM) and FM → FM transitions yield a GMR effect, whereas for magnetic fields above the saturation of the FM regions, only the FM → SPM and SPM → FM transitions remain effective with regard to GMR. The strong mixing effect of the simultaneous Co dissolution and Cu deposition could contribute to the formation of such interfacial loose-spin regions, but the problem remains how to decouple them magnetically from the FM core of the magnetic layers. A decoupling can occur via a non-magnetic (Cu-enriched) region or due to the reduced exchange coupling between interfacial magnetic spins with respect to the interaction between atoms in the FM core.

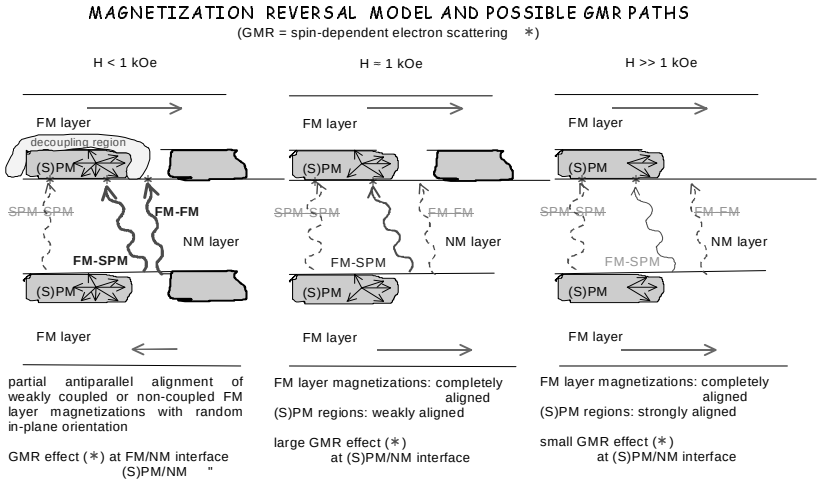

Fig. 4. Schematic cross-sectional view of a magnetic/non-magnetic multilayer in which the magnetic layer is consists mainly of FM regions but there are superparamagnetic (SPM) or paramagnetic (PM) regions in the interfaces between the magnetic and non-magnetic layers. The horizontal arrows indicate the magnetization orientations of the FM layers for low, intermediate and high fields (the shorter arrow in the lower FM layer is for showing an eventual partial antiparallel alignment). The star-like arrows refer to the random temporal fluctuations of the (S)PM magnetic moments which graudally align with increasing magentic fields. The wavy arrows display possible electron paths leading to a GMR effect (✱): the thickness of the solid arrow lines indicates the magnitude of GMR and the dashed arrow lines refer to ineffective paths (in our samples, SPM-SPM paths at all fields and FM-FM paths for magnetic fields beyond the saturation of the FM magnetization).

Unfortunately, the present experiments do not allow to decide between the possible spatial arrangements for the SPM regions and, clearly, further sophisticated local structure and chemical analysis techniques are involved for unraveling this problem.

5. Summary

In this paper, we discussed the GMR behaviour of magnetic/non-magnetic multilayers in the case when the magnetic layers are not fully ferromagnetic, but contain also regions exhibiting SPM characteristics. According to the Wiser-Hickey model [16,17], in such cases the GMR may contain, besides the usual GMR_{FM} term, also a contribution GMR_{SPM} with a strong field dependence described by the Langevin function L(x) which arises from spin-dependent scattering events involving a FM region and a SPM region.

As a particular example, the magnetoresistance and magnetic properties were studied for two electrodeposited Co-Cu/Cu multilayers prepared with identical nominal magnetic layer thicknesses, but with strongly differing nominal non-magnetic layer thicknesses. For both multilayers, the GMR could be decomposed into a FM and a SPM term along the lines of the Wiser-Hickey model. However, there were striking differences between the two multilayers in that the GMR_{FM} term dominated in one multilayer and the GMR_{SPM} term in the other one. In the latter case, the average size of the SPM regions derived from both GMR and magnetization data was found to be about half of the value obtained for the former multilayer.

The striking differences were explained by taking into account the way in which the Co dissolution process during the Cu deposition cycle can influence multilayer growth under the specific deposition conditions applied. Studies based on a similar decomposition analysis of the GMR may further help in clarifying the detailed influence of deposition conditions on multilayer formation. It should be noted that such a decomposition analysis may well be applied also to multilayers prepared by other techniques.

Low temperature magnetic and magnetoresistance measurements are in progress on the two samples investigated here with the aim of getting further information on the SPM regions in these multilayers.

Acknowledgements

This work was supported by the Hungarian Scientific Research Fund (OTKA) through grants F 032046 and T037673 and by the Deutsche Forschungsgemeinschaft (DFG), Germany through Sonderforschungsbereich 422.

References

[1] P. Grünberg, Acta Mater. **48**, 239 (2000).
[2] I. A. Campbell, A. Fert, Transport Properties of Ferromagnets. In: Ferromagnetic Materials, Vol. **3**, Ch. 9, ed. E.P. Wohlfarth (North-Holland, Amsterdam, 1982).
[3] J. Mathon, Contemp. Phys. **32**, 143 (1991); D. M. Edwars, J. Mathon, R. B. Muniz, IEEE Trans. Magn. **27**, 3548 (1991).
[4] M. N. Baibich, J. M. Broto, A. Fert, F. Nguyen Van Dau, F. Petroff, P. Etienne, G. Creuzet, A. Friederich, J. Chazelas, Phys. Rev. Lett. **61**, 2472 (1988).
[5] G. Binasch, P. Grünberg, F. Saurenbach, W. Zinn, Phys. Rev. B **39**, 4828 (1989).
[6] S. S. P. Parkin, N. More, K. P. Roche, Phys. Rev. Lett. **64,** 2304 (1990).
[7] D. H. Mosca, F. Petroff, A. Fert, P. A. Schroeder, W. P. Pratt Jr., R. Laloee, J. Magn. Magn. Mater. **94**, L1 (1991).
[8] H. Kubota, S. Ishio, T. Miyazaki, Z. M. Stadnik, J. Magn. Magn. Mater. **129**, 383 (1994).

[9] A. E. Berkowitz, J. R. Mitchell, M. J. Carey, A. P. Young, S. Zhang, F. E. Spada, F. T. Parker, A. Hutten, G. Thomas, Phys. Rev. Lett. **68**, 3745 (1992).
[10] J. Q. Xiao, J. S. Jiang, C. L. Chien, Phys. Rev. Lett. **68**, 3749 (1992).
[11] C. L. Chien, Mater. Sci. Eng. B **31**, 127 (1995).
[12] B. D. Cullity, Introduction to Magnetic Materials (Addison-Wesley, Reading, 1972).
[13] T. Shinjo, in: Magnetism and Structure in Systems of Reduced Dimensions. Ed. R.F.C. Farrow et al. (Plenum Press, New York, 1993), p. 323.
[14] J. L. Gittleman, Y. Goldstein, S. Bozowski, Phys. Rev. B **5**, 3609 (1972).
[15] S. Zhang. Appl. Phys. Lett. **61**, 1855 (1992).
[16] N. Wiser, J. Magn. Magn. Mater. **159**, 119 (1996).
[17] B. J. Hickey, M. A. Howson, S. O. Musa, N. Wiser, Phys. Rev. B **51**, 667 (1995).
[18] B. J. Hickey, M. A. Howson, S. O. Musa, G. J. Tomka, B. D. Rainford, N. Wiser, J. Magn. Magn. Mater. **147**, 253 (1995).
[19] J. Xu, B. J. Hickey, M. A. Howson, D. Greig, R. Cochrane, S. Mahon, C. Achilleos, N. Wiser, Phys. Rev. B **56**, 14602 (1997).
[20] T. Lucinski, F. Stobiecki, D. Elefant, D. Eckert, G. Reiss, B. Szymanski, J. Dubowik, M. Schmidt, H. Rohrmann, K. Roell, J. Magn. Magn. Mater. **174**, 192 (1997).
[21] I. Bakonyi J. Tóth, L. F. Kiss, E. Tóth-Kádár, L. Péter, A. Dinia, J. Magn. Magn. Mater. **269**, 156 (2004).
[22] I. Bakonyi, L. Péter, Z. Rolik, K. Kiss-Szabó, Z. Kupay, J. Tóth, L.F. Kiss, J. Pádár, to be published.
[23] T. R. McGuire, R. I. Potter, IEEE Trans. Magn. **11**, 1018 (1975).
[24] V. Weihnacht**,** L. Péter, J. Tóth, J. Pádár, Zs. Kerner, C.M. Schneider, I. Bakonyi, J. Electrochem. Soc. **150**, C507 (2003).
[25] L. Péter, Á. Cziráki, L. Pogány, Z. Kupay, I. Bakonyi, M. Ahlemann, M. Herrich, B. Arnold, T. Bauer, K. Wetzig, J. Electrochem. Soc. **148**, C168 (2001).
[26] L. Péter, Q. X. Liu, Zs. Kerner, I. Bakonyi, Electrochim. Acta **49**, 1513 (2004).
[27] W. R. A. Meuleman, S. Roy, L. Péter, I. Varga, J. Electrochem. Soc. **149**, C479 (2002).
[28] Q. X. Liu, L. Péter, J. Tóth, L. F. Kiss, Á. Cziráki, I. Bakonyi, J. Magn. Magn. Mater. (2004), in press.